

Rehabilitation of two Centenary buildings located in the historic district of Baixa Pombalina, in Lisbon

Laura Pacheco

Department of Civil Engineering, Instituto Superior Técnico, Technical University of Lisbon, Portugal

May 2018

Abstract : The rehabilitation of centenary buildings located in Lisbon downtown, more precisely, in the historic district of “Baixa Pombalina” has taken, from the last decades, an important role in the revitalization of this historic district. The grade of degradation of the buildings and the deficient or completely lack of conditions considering nowadays use, or even, when a new use is defined, are major factors regarding the type of rehabilitation process to be implemented, including, more or less intrusive measures. Nevertheless, for both situations, the new charges or the increase of the existing ones, determines the need for the reinforcement of the existing foundations. Also, in this historic district, the subsoil is a concern, as it is characterized by the presence of alluvium deposits throughout a considerable depth over the Miocene bedrock. So, the foundation reinforcement solution must provide the necessary load transfer, essentially through lateral friction, what allied to the space restraints, are relevant for the selection of the equipment and the design solution. In this context micropiles solutions have a greatest value. The predesign for micropiles, is usually checked by previous micropile load test(s), in real scale, and, both the design and construction process are verified by instrumentation and monitoring in an active way.

KEYWORDS: Foundations reinforcement, Micropiles, Load test, Backanalysis, Instrumentation

1. Introduction

The rehabilitation of old buildings in historic districts has been a major challenge in the revitalization of these areas. The deterioration level and the lack of the necessary conditions to nowadays use are the main factors for the type of rehabilitation, with more or less impact on the original building. The more intrusive ones, includes the demolition of all the interior of the building conserving only the existing historic facade(s). When less intrusive measures are assumed, only a global or punctual rehabilitation process is undertaken. The new loads, the eventual establishment of underground facilities, the vicinities, the groundwater level, the lithology of the subsoil, the architectural or historic elements to preserve, usually determines the geotechnical

design solution to be implemented. In this context, micropiles have a greatest value, as they are especially suitable where the ground conditions are very variable, where the access is restrictive, where structural movements in service must be minimum, or even when environmental pollution aspects are significant. The rehabilitation of the centenary buildings addressed in this paper is an example where almost of those aspects were determinant. The buildings are located in Lisbon downtown, more precisely, in the historic district of “Baixa Pombalina”. The rehabilitation process involved, in one of them, the total demolition of the interior and the back facade, preserving the original frontal facade, in the other one, the original structure was maintained, nevertheless the additional loads due to the new use and design requirements, imposed the

reinforcement of the existing foundations. For both cases, the new foundations and the reinforcement of the original foundations, design solutions were materialised by micropiles. To validate the predesign solution, a micropile tension load test, in real scale, was performed at site. Also, both design and construction process, were verified by instrumentation and monitoring in an active way. The load test was the basis for the backanalysis of the geotechnical properties of the soil discussed here in, and, the instrumentation measurements were analysed, in the context of the backanalysis of the performance of the design solutions.

2. Case study

The site work is located in the district of Baixa Pombalina, in Lisbon. The buildings confront with Prata Street and Correeiros Street, as it can be seen in the aerial view of Figure 1.



Figure 1 – Aerial view of the intervention site (Google Earth).

The two buildings confront each other by an open space at the back facades (Figure 2).

The rehabilitation process included the demolition of all of the interior of the building that confronts with Prata street (Building 1),

conserving only the existing historical front façade, and, global rehabilitation measures on the building that confronts with Correeiros street (Building 2), maintaining its original structural elements.

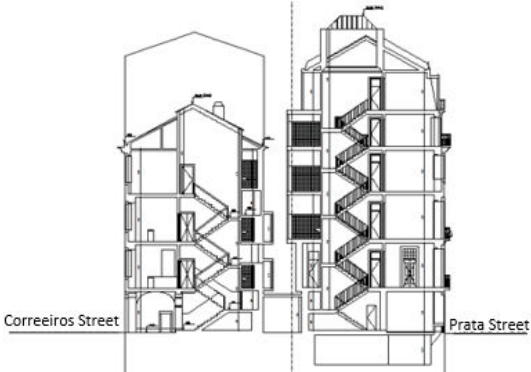


Figure 2 – Cross section throughout the buildings before the rehabilitation works.

The buildings are to be connected, in order to create the future “Hotel da Baixa”. The foundation designed solution included reinforcement of the original foundations and new indirect foundations, with micropiles. The designed solutions, are shown in Figure 3 and Figure 4, for each building.



Figure 3 - Designed foundations plant for Building 2 (JETSJ, 2016).

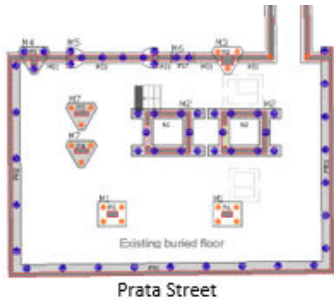


Figure 4 - Designed foundations plant for Building 1 (JETSJ, 2016).

The micropiles were self-drilling Ø200mm, materialized by hollow steel tubes type N80 (API 5A), whose section and length differed from each building: Ø88,9x7,5mm with 20m length at Buildings 1 and 2 (orange colour), and Ø127x9mm with 25m length at Building 1 (blue colour), respecting to Figures 3 and 4.

3. Geologic / Geotechnical / Hydrogeologic scenario

The geologic environment of the intervention site is shown in Figure 5. The area is characterized by a vigorous layer of alluvium deposits (a) that lays over the Miocene bedrock (M). This sequence is covered by a superficial landfill of anthropogenic deposits (At).

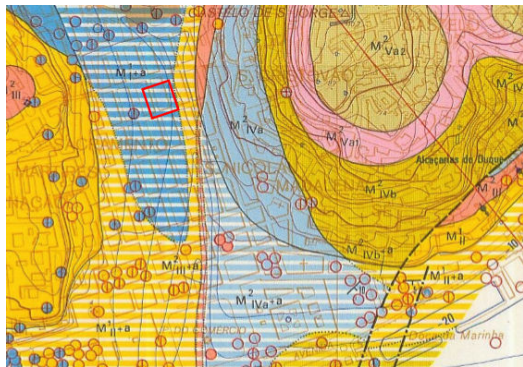


Figure 5 – Intervention site in the Geologic map of Lisbon

The alluvium deposits, are composed by lenticular bodies and significant lateral and vertical facies variation. The lithological facies include soft to hard silt and clay, and loose to dense sands. Regarding to the anthropogenic deposits, they include the debris of 1755 earthquake. The subsoil of the intervention site was investigated, through 3 geotechnical boreholes that included SPT's performed each 1,5m. The distribution of the boreholes (S1, S2 and S3) is shown in Figure 6.

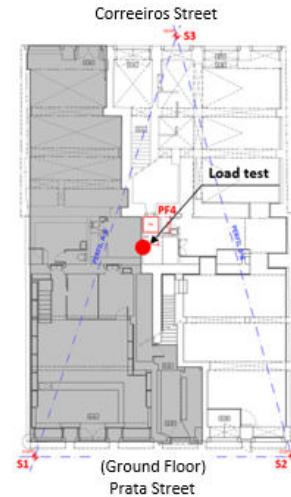


Figure 6 - Spatial distribution of geotechnical boreholes and approximate location of the load test

The logs from the 3 geotechnical boreholes were analysed. The results of the SPTs values vs. depth, denoted to different resistant profiles of the soil, and have clearly highlighted the depth of the over consolidate Miocene bedrock (Figure 7). The static water level was detected about 4m depth from the ground floor.

A geophysical approach based on the $N_{SPT}-V_s$ correlations, validated in Teves Costa *et al.* (2014), related to a geophysical study for downtown formations, allowed to estimate the initial rigidity of the soil, on the basis of which the backanalysis was developed. Those correlations (Table 1), from Dikmen (2009), for the anthropogenic deposits and the alluvium deposits, and from Lee (1990), for the Miocene formations, were validated in the referred study, for downtown central zone, which corresponds to the present intervention area. In the same paper, are considered the correlations for the specific weigh (γ) with N_{SPT} values, proposed by Boules (1982), in the form:

$$\gamma = 2\ln(N_{SPT}) + 12.1 \text{ (alluvium deposits)}$$

$$\gamma = 2,1\ln(N_{SPT}) + 11 \text{ (anthropogenic deposits)}$$

Considering these correlations, the initial distortional modulus (G_0) was estimated for the 3 profiles earlier defined. Through the elastic relations the values for E_0 were obtained.

Table 2 shows the values thereby obtained, for the 3 profiles, in an identical geometrical model estimated for the site of the load test.

Table 1 – Correlations N_{SPT} - V_s from Dikmen (2009) and Lee (1990) for the different types of soil and stratigraphically.

Correlation	α	β	Material	Author	Unit
$V_s = \alpha N_{SPT}^\beta$	58	0,39	Undifferentiated	Dikmen (2009)	Anthropogenic deposits
	73	0,33	Sand	Dikmen (2009)	Sandy alluvium
	57	0,49	Sand	Lee (1990)	Miocene Formations

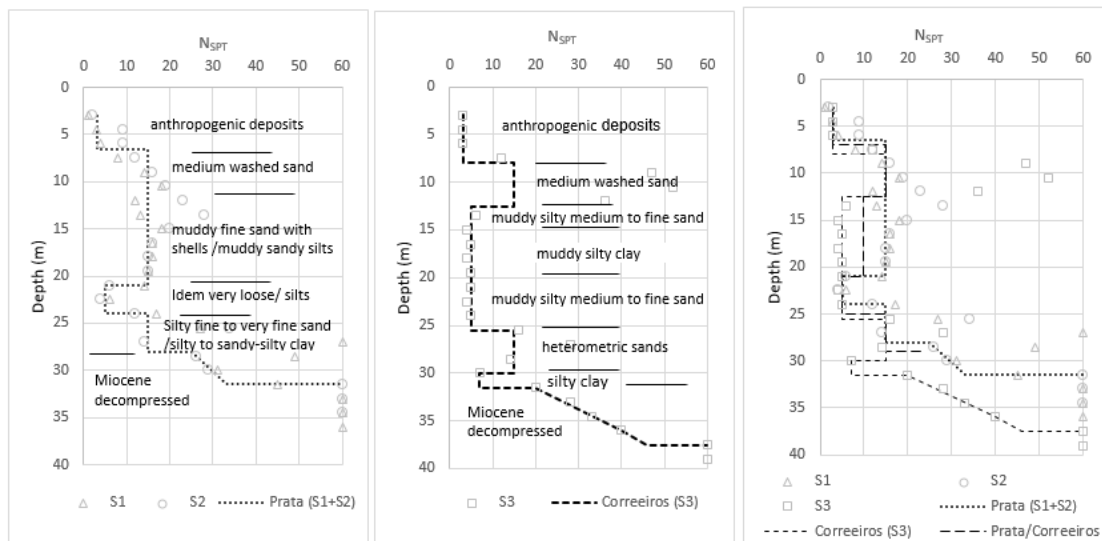


Figure 7 - Graphic of SPT values vs. depth and estimated type profiles.

Table 2 – Estimated values for specific weigh of the soil (γ) and initial soil modulus (E_0) for the for the different soil profiles.

Soil profile / Type		Prata			Correeiros			Intermediate		
Geologie	Prof (m) Zi Zf	N_{SPT} (-)	γ (kN/m3)	E_0 (MPa)	N_{SPT} (-)	γ (kN/m3)	E_0 (MPa)	N_{SPT} (-)	γ (kN/m3)	E_0 (MPa)
Anthrop. Dep.	< 7,0	3	13,4	26	3	13,3	26	3	13,3	26
Alluvium	7,0 12,0	15	17,5	136	15	17,5	136	15	17,5	136
	12,0 21,5	5	15,3	58	5	15,3	58	5	15,3	58
	21,5 25,5	5	15,3	58	5	15,3	58	5	15,3	58
	25,5 29,0	15	17,5	136	15	17,5	136	15	17,5	136
Miocene	> 29	-	-	-	-	-	-	-	-	-

4. Site restraints

The first conditioning in a geotechnical project is the geological and geotechnical, seismic, and hydrogeological scenario, and it was the issue of the previous chapter. Nevertheless, it is important to sign that the depth of the water level has contributed to prevent the opening of a second buried floor. Here in, the main work restraints will be focused. The photographs

shown here in were obtain by the author during the works follow-up.

Vicinity restraints

The buildings confront laterally with other buildings from the same age. The depth of existing foundation was investigated considering the execution of 3 manually excavated wells localized near the masonry walls of the buildings, namely PF4 (Figure 6), on the ground floor of the

open area between the two buildings, and the two others, PF2 and 3, executed from the existing buried floor of the Building 1. The depth of the existing masonry foundations was detected at about 3,5m from the ground floor. Also, the adding of new floors without apparent foundation reinforcement is a site conditioning.

Restraints related to constructive aspects and the architectural definition

These ones are related to the rigorous sequence of works that must be followed in a demolition and façade retention is performed (Figure 8).

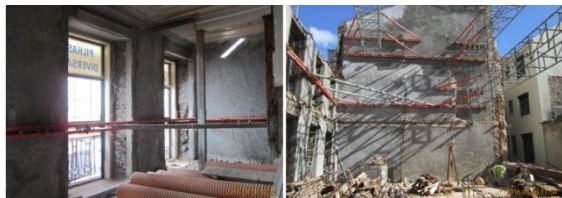


Figure 8- Photos of the demolition and façade retention processes.

Restraints related to the archaeological heritage (buried)

The restraints related to these aspects were the various order, in instance it was detected an old system of sewerage, cloaca, during the excavation works of the façade foundation in Building 1 (Figure 9). Also, an archaeological dig at Building 2 shown evidences of pre-Pombaline construction.



Figure 9 – System of sewerage, cloaca.

Restraints related to the accessibilities

The execution of works in limited spaces and near structural elements is shown in Figure 10.



Figure 10 - Limited spaces / structural elements.

Restraints related to the contract term

For the majority of the construction works, sometimes the safety concerns are disregarded due to this conditioning (Figure 11).



Figure 11 – Examples of disregarded security concerns due to the execution time conditioning.

Also, due to this conditioning, the micropiles executed for the peripheral reinforcement of façade foundation of Building 1, have a different spacing because of the system of sewerage shown in Figure 11. The approval for demolition was not waited.

Restraints related to site construction

In rehabilitation works the areas for the stock of materials and other facilities are limited, so the building itself is used for that effect (Figure 12).



Figure 12 - Examples of site construction restraints.

5. Backanalysis of soil properties

The backanalysis of the geotechnical properties of soil was based on a load test performed to a micropile, at the work site (Figure 6). Here in, the load test will be introduced, followed by the expedite method applied, and finally the approach by finite elements (Plaxis 2D).

Load test

The load test was executed according to the European Standard EN1537, for ground anchors (traction loads). The graphic representation is shown in Figure 13 (values of load – displacement in Table 3).

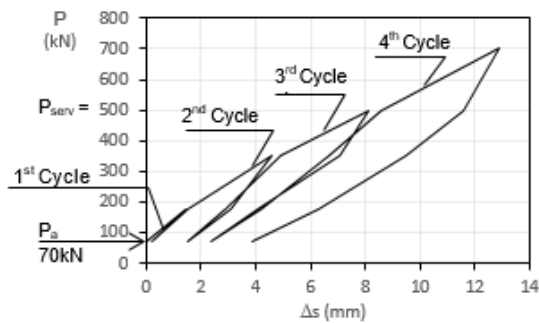


Figure 13 – Load-displacement curve of the load test

The maximum load ($P_p=700\text{kN}$) was defined for 1,4 times the service load ($P_{serv}=500\text{kN}$), without mobilizing a rupture situation. A preload of 10% P_p ($P_a=70\text{kN}$) was applied without readout of related displacement.

Table 3 – Values of load – displacement (load test)

Cycle	P (kN)	Displacement (mm)								
		70	175	70						
1st Cycle	70	0	1,45	0,2						
2nd Cycle	P (kN)	70	175	350	175	70				
	Δ (mm)	0,2	1,5	4,6	3,1	1,5				
3rd Cycle	P (kN)	70	175	350	500	350	175	70		
	Δ (mm)	1,5	2,9	4,9	8,1	7,1	4,1	2,4		
4th Cycle	P (kN)	70	175	350	500	700	500	350	175	70
	Δ (mm)	2,4	4,2	6,7	8,6	12,9	11,6	9,5	6,3	3,9

The micropile was executed using self-drilling technology, with steel tubes N80 (API 5A) with the characteristics defined in Table 3. To allow the application of traction loads, a high

resistance steel bar $\varnothing 32\text{mm}$ (Table 4) was sealed in his interior.

Table 4 – Characteristics of the steel elements

Type	f_y (MPa)	f_u (MPa)	E_t (GPa)	A_t (m ²)
N-80 $\varnothing 88,9 \times 7,5\text{mm}$	560	703	210	1,918E-03
Steel bar A950/1050 $\varnothing 32\text{mm}$	764	844	205	8,040E-04

The geometric characteristics of micropile N80 and the steel bar are shown on Table 5. The micropile was firstly executed with 20m depth from the ground floor, and latter a 4m hole was excavated to allow the implantation of a crane. So, the micropile was cut above the cap.

Table 5 – Geometric characteristics of the micropile: free length (L_{tf}); fixed length (L_{tb}), supplementary length (L_e – between anchor head and anchorage point at jack)

Steel	i (°)	$L_{tf} = L_{free}$ (m)	$L_{tb} = L_{fixed}$ (m)	L_e (m)
N-80 $\varnothing 88,9 \times 7,5\text{mm}$	90	2	16	0
Varão $\varnothing 32\text{mm}$ (A950/1050)	90	2	n.a.	0,8

The apparent free length was calculated considering only the steel tube N80 (scenario 1), and including also the steel bar (scenario 2). Free length limits for each scenario, were calculated, and plotted against the elastic displacements (Figure 14), as an anchor test procedure.

During the load test, the displacement measurements at the maximum load of each cycle, didn't reveal fluence.

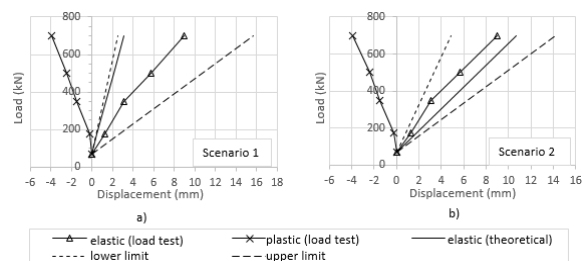


Figure 14 – Graphic of elastic and plastic displacements and elastic limits of the free length for both scenarios.

Expedite methods

- Load test simulation as a ground anchor (Carvalho, 1996)

In order to estimate the ultimate load of the micropile, the method proposed by Carvalho, to simulate reception anchor tests, was applied, and both scenarios were studied.

To estimate the parameters characteristics of the resistance and rigidity of the interface bulb-soil, this is, the maximum distortional modulus (G_0) and the ultimate shear stress (τ_{ult}) mobilized at the interface, the following steps were performed: 1) representing the load phases and the unload phases separately; 2) reset the load phases of each load cycle; 3) estimate the mobilized displacement on soil, in the interface zone, at the end of each load increment

$$\delta_e = \Delta P \cdot (L_{app})_{middle} / (E_t A_t)$$

$$\delta_{soil} = \delta p = \delta t - \delta e$$

4) Convert the diagram of applied load (P-Pi) vs. displacement (δ_{soil}), in the diagram of applied shear stress (τ - τ_i) vs. distortion (γ), dividing by the lateral area of the bulb for shear and dividing the bulb diameter for distortion; 5) estimate the ultimate shear stress (τ_{ult}) and the initial distortional modulus ($G_{m\acute{a}x}$) by linear regression through the graphic of ($\gamma/(\tau-\tau_i)$; γ). The equation of the tendency line is in the form of $y=m.x+c$, being \underline{m} the inverse value of $(\tau-\tau_i)_{ult}$, and \underline{c} is the inverse of G_0 . Knowing τ_i , which is obtained applying the same procedure. The application of method conduced to the results shown in Table 6, for both scenarios.

Table 6 – Estimated parameters for both scenarios ($R_f=1$; $P_{ult}=Prot$).

Sc.	$(\tau_{ult} - \tau_a)$ (kPa)	τ_a (kPa)	τ_{ult} (kPa)	G_t (MPa)	P_{ult} (kN)	SSL (-)	$G_{m\acute{a}x}$ (MPa)
1	110,2	6,96	117,2	16,4	1178	0,059	18,5
2	91,4		98,4	28,6	989	0,071	33,1

Considering the estimated parameters of Table 6, both scenarios were simulated (Figure 15) and the best compared results, considering the unload-reload behavior expressed by G_{sec} , was achieved for scenario 1.

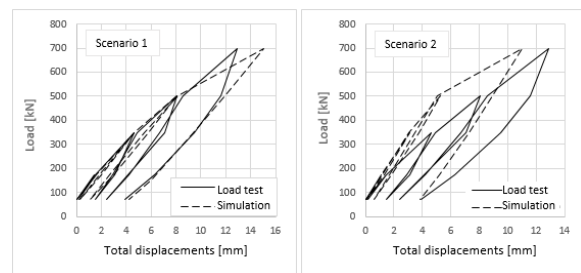


Figure 15 – Load test simulation for both scenarios.

So, for scenario 1: $L_e=0$, $L_{tf}=2,0m$ (micropile cap), $L_{tb}=16m$, and the steel element considered is only the tube N80 (API 5A). The final estimated parameters based on Carvalho's method, are then: $(q_s)_{ult}=\tau_{ult}=117,2kPa$, $P_{ult}=1178kN$, $G_0=18,5MPa$. In parallel with Bustamante method for predesign, $(q_s)_{ult}$ corresponds to a limit pressure of about 625kPa for sands and 375kPa for silt and clays.

- Ultimate load according to Chin (1970/1972)

The method proposed by Chin was developed for load tests on piles. This method is based on the hyperbolic representation of the results of the load test in the form of Δ/P vs. Δ , in order to obtain the best regression line for those points, whose gradient is the inverse of the ultimate load (P_{ult}), being Δ the total displacement. As the displacement for the initial load increment (0-70kN) wasn't known, it was admitted an elastic displacement corresponding to L_{tf} . The ultimate

load was estimated considering the last 3 and 4 points of the curve, obtaining the following values: 1761kN and 1350kN.

➤ Load test simulation by Fleming (1996)

Regarding Fleming method, the displacement is estimated as the sum of the component corresponding to the lateral friction (Δ_S) and the elastic component (Δ_E), for a floating pile :

$$\Delta_S = \frac{M_S D_S P_S}{U_S - P_S}$$

$$\Delta_E = \frac{4}{\pi} \times \frac{P(L_0 + K_E \times L_F)}{D_S^2 \times E_c}, \quad P_T \leq U_S$$

M_S is a flexibility factor. The axial rigidity of the materials is defined in Table 7 and characteristics of the micropile are shown in Table 8. The lowest value of the flexibility factor (M_S) that allowed to adjust at least one of the ultimate load scenarios was 0,05, as shown in Figure 16.

Table 7 – Micropile materials properties

Materials	Section mm	A m ²	E kN/m ²	EA kN/m
Tube N80	Ø88,9x7,5	1,918E-03	2,10E+08	4,028E+05
Grout	Ø200	2,950E-02	2,100E+07	6,195E+05

Table 8 – Characteristics of the micropile

Pile	L _{Total}	L ₀	L _F
L (m)	18	2	16
EA (kN/m)	-	4,028E+05	3,254E+07

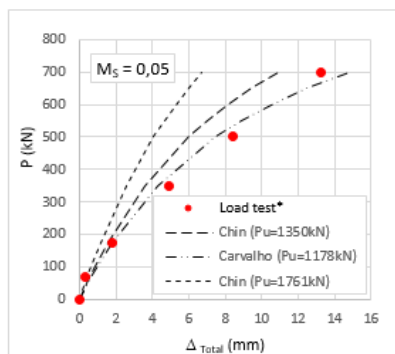


Figure 16- Simulations of the load test $K_E=0,4$ (Fleming method).

The displacement values from the load test were corrected for the load increment 0-70kN, like as for Chin method. The value of P_{ult} obtained through Carvalho's method, 1178kN, was the best option here in. The biggest value of $P_{ult,Chin}$ has shown to be completely out of range.

➤ Load test simulation by Mayne and Schneider (2001)

This method uses the dynamic concept of the degradation of soil rigidity with the level of applied load, from the range of very low displacements to large displacement range (engineering works), considering for this propose the equation of Fahey and Carter (1993). This equation is then introduced in the equation of Poulos (1987,1989) for settlement calculations, as:

$$w_t = \frac{Q \cdot I_p}{d \cdot E_{m\acute{a}x} \cdot [1 - f(Q/Q_{ult})^g]}$$

Where Q is the applied load, Q_{ult} is the axial capacity under loading, f and g are hyperbole parameters (f = 1.0; g = 0.3), and I_p is the settlement influence factor expressed by the concise form of Randolph e Wroth (1978). I_p is defined for the conditions of the micropile, floating, and the soil $E_{sL}/E_b =$ (soil modulus along pile shaft at level of base/ soil modulus bellow foundation base) =1, and being actualized for each calculation step.

The simulations were performed considering $P_{u,Carv} = 1178\text{kN}$ and $P_{u,Chin} = 1350\text{kN}$. For E_0 , was considered the weighted average from the estimated values shown in Table 2, except for the initial layer of landfill, being neglected. The values of load test displacements were corrected (Δ^{**}) in each simulation:

$$\Delta^* = \Delta_{ensaio} + (\Delta_{Ltf})_{70} \rightarrow \Delta^{**} = (\Delta^* - \Delta_{Ltf}) + (\Delta_{70})_{\omega t}$$

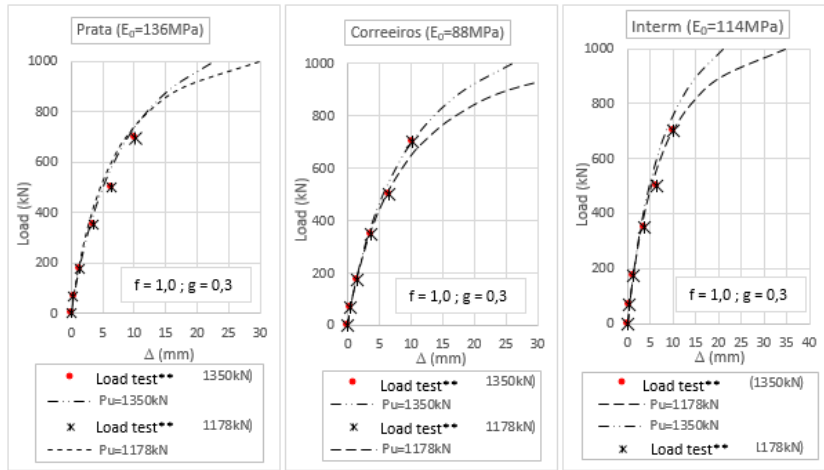


Figure 17 - Load test simulations (Mayne and Schneider method).

As shown in Figure 20 the best adjustment is obtained for weaker soils and $P_{ult}=1178$ kN.

Backanalysis through Plaxis 2D

Based on last results (weaker soil profiles), the load test was then simulated through the software Plaxis 2D v8.6 (axisymmetric model), and the soil behaviour modelled by the Hardening Soil model with small strain stiffness (HSs) for the alluvium deposits and Mohr-Coulomb model (M-C) for the anthropogenic deposits. The box was set with 16m width and 29m height, and standard displacement limit conditions. E_{ref} was estimated from E_0 , based on the degradation law, for the service load level (500kN), with $Q_{ult} = 1178$ kN

On HSs model, it was assumed: $E_{50} = E_{ur} / 3$, being E_{ur} equal to the secant degraded modulus, $E_{50} = E_{oed}$, and $\gamma_{0,7}$ is estimated through the equation:

$$\gamma_{0,7} \approx \frac{1}{9G_0} [2c'(1 + \cos(2\varphi')) - \sigma'_1(1 + K_0) \sin(2\varphi')]$$

Five distinct layers were considered, from the surface to the admitted depth of top of Miocene formations, at the load test site (29m). First layer (0-7m) corresponding to the anthropogenic deposits and the remaining ones (7-29m)

corresponding to the alluvium deposits. The water table was set at 4m depth. The estimated values of geotechnical parameters for Plaxis simulations are shown in Table 9. The shear angle was estimated mainly through local correlations proposed in Silvério Coelho (1996): $\phi' = 24 + 13\log(N_{SPT}/A)$. Where, A takes the value of 5 for clays, 2,5 to fine to medium sand, silty or muddy, and 1 for clayey sands or rough medium sands. The correction of the displacements was updated for load level of 70kN of Plaxis.

The simulations shown in Figure 18 denoted a very good adjustment with the load test allowing to estimate the soil properties (layer 3), of resistance in a range of $6 < N_{SPT} < 10$, and rigidity between $5,1 < E_s < 7,5$ MPa, with a best fit, from the author's perspective, of about $N_{SPT} = 8$ and $E_s = 6,3$ MPa.

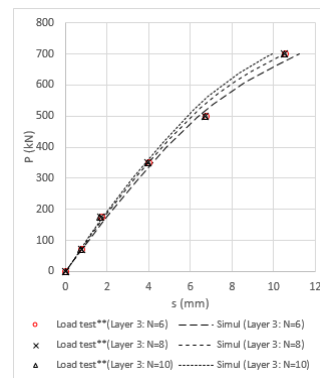


Figure 18 - Load test simulations through Plaxis 2D

Table 9- Estimated values of geotechnical parameters for Plaxis simulations

Layers	1		2		3 (N=10)		3 (N=8)		3 (N=6)		4		5	
	Fill		Alluvium											
Model	M-C	Hs	Hs	Hs	Hs	Hs	Hs	Hs	Hs	Hs	Hs	Hs	Hs	Hs
	Undrained	Drained	Drained	Drained	Drained	Drained	Drained	Drained	Drained	Drained	Drained	Drained	Drained	Drained
γ_{sat} (kN/m ³)	13,5	17,5	16,7	16,3	15,7	15,3	17,5							
γ_{sat} (kN/m ³)	14	17,5	16,7	16,3	15,7	15,3	17,5							
$k_v=k_h$ (m/dia)	0,009	0,138	0,138	0,138	0,138	0,138	0,138							
$E_{s(undr)}$ (MPa)	5,8	10,3	7,5	6,3	5,1	4,4	10,3							
$E_{s(drained)}$ (MPa)	-	10,3	7,5	6,3	5,1	4,4	10,3							
$E_{u(drained)}$ (MPa)	-	30,9	22,6	19,0	15,2	13,1	30,9							
c_{int} (kPa)	5	0,2	0,2	0,2	0,2	0,2	0,2							
ϕ (°)	21	35	31	30	28	27	34							
ψ (°)	0	5	1	0	0	0	4							
ν (-)	0,35	-	-	-	-	-	-							
ν_{ur} (-)	-	0,2	0,2	0,2	0,2	0,2	0,2							
m (-)	-	0,5	0,5	0,5	0,5	0,5	0,5							
$\gamma_{b,z}$ (-)	-	0,0002	0,0005	0,0005	0,0006	0,0010	0,0005							
G_0 (MPa)	-	56,8	41,5	35,0	27,9	24,1	56,8							

6. Analysis of the designed solution

The instrumentation included 8 topographic targets, 4 in each facade. The alert and alarm triggers were defined in the project at displacements of 10 and 15mm, respectively. In Building 2 the maximum displacements were at about 5mm. Regarding to Building 1, the horizontal (ΔP) and the vertical (ΔZ) displacements, accused larger values, as shown on Figure 19. These displacements, specially the horizontal displacement (ΔP) registered at the topographic target 3, concerns to demolition and implementation of the bracing system. The vertical ones, may be attributed to some load transfer occurred Nevertheless, it has stabilized near the alert trigger.

7. Main conclusions

The following main conclusions can be highlighted:

- The restraints associated with the foundations reinforcement work, followed up during most of the construction phases, took on particular importance, in the choice of the design solution itself, in the choice of equipment, in the execution sequence, in the management of spaces, in all aspects related to safety;
- The analysis of the geological-geotechnical, hydrogeological and seismic scenario of the site, together with the use of correlations with local

expression, allowed to obtain good results throughout the study carried out for the backanalysis of soil geotechnical properties;

- The expedited methods used in the simulation of the load test allowed to estimate a probable value for the ultimate load and to restrict the possibilities regarding to the soil characteristics, before the analysis through finite elements with software Plaxis 2D;

- This model allowed to define trigger values for displacements: 6 and 10mm, corresponding to service load and maximum load (considering a soil profile with similar characteristics to those estimated for the test site).

References

- Carvalho, M. R. (2009). *Ancoragens pré-esforçadas em obras geotécnicas. Construção, ensaios e análise comportamental*. FEUP.(in portuguese)
- Chin Fung Kee. (1972). *The inverse slope as a prediction of ultimate bearing capacity of piles. Proceedings, 3rd SE Asia Conference on Soil Engineering*, (pp. 83-91). Hong Kong.
- Fleming, W. K. (1992). *A new method for single pile settlement prediction and analysis. Géotechnique 42, No. 3*, pp. 411-425.
- Geocontrole - Geotecnia e Estruturas de Fundação, S.A. (2015). *Estudo Geológico-Geotécnico*. (in portuguese)
- JetSJ Geotecnia, Lda. (2016). *Projecto de Fundações*. (in portuguese)
- Mayne, P. W., & Schneider, J. A. (2001). *Evaluating axial drilled shaft response by seismic cone. Foundations & Ground Improvement, Geot. Sp. Pub. GSP 113, ASCE*, 655-669.
- Silvério Coelho. (1996). *Tecnologia de Fundações*. EPGE. (in portuguese)
- Teves Costa et al. (2014). *Geotechnical characterization and seismic response of shallow geological formations in downtown Lisbon. Annals of Geophysics, Istituto Nazionale di Geofisica e Vulcanologia INGV - ISSN: 2037-416X*, 24.